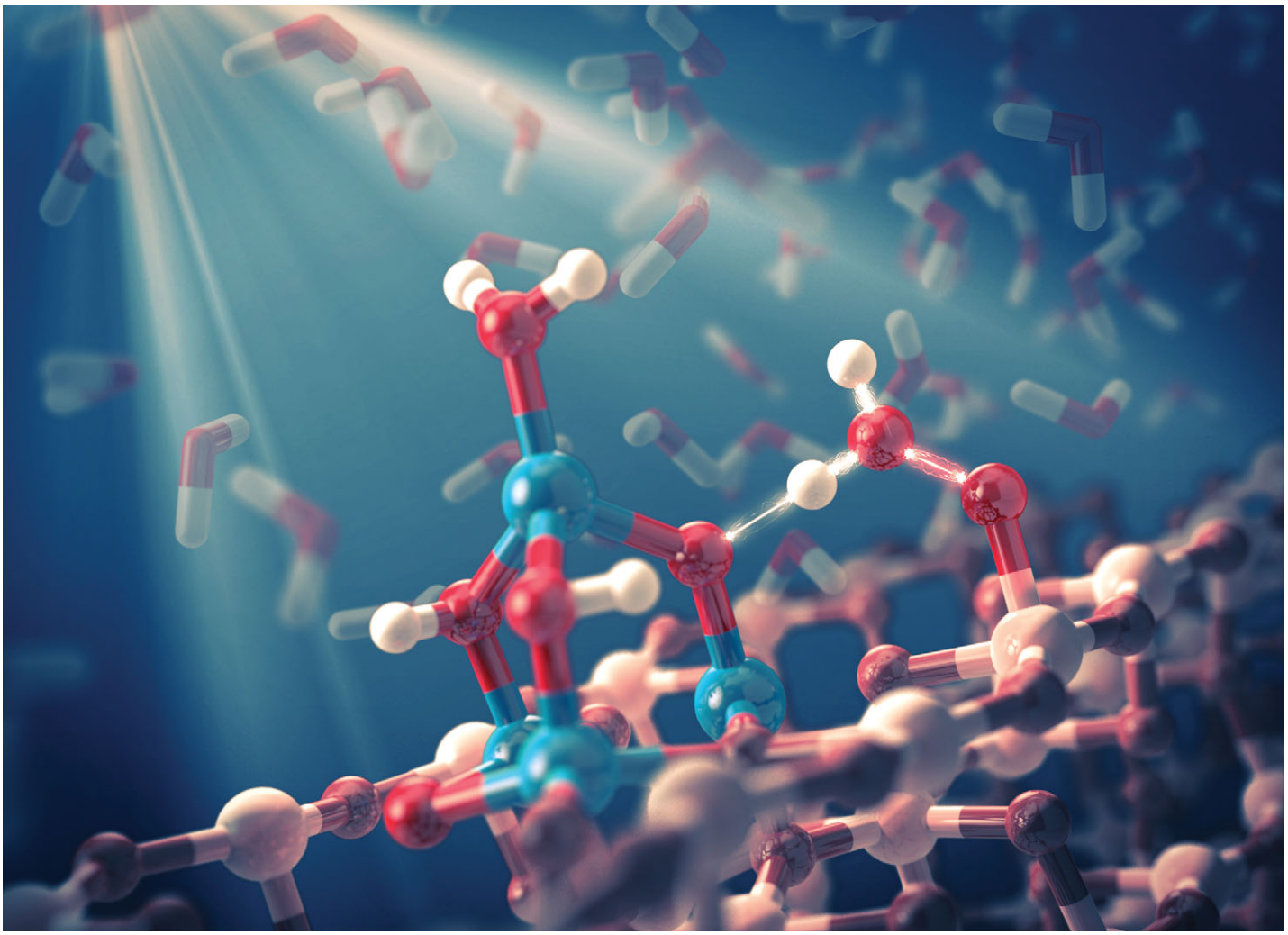

The work has been initiated at the Institute for Complex Molecular Systems, Eindhoven University of Technology (The Netherlands) and continued in collaboration with Institute for Solid State Theory, University of Muenster (Germany).

Title: Synergy between TiO_2 and Co_xO_y sites in electrocatalytic water decomposition

The water electrolysis process requires the use of the proper catalyst in order to lower the overpotential needed to overcome the thermodynamic limitations of the process. The study presented in the article makes use of the MD simulation with explicit solvent to evaluate the relative stability of the particular intermediates in the electrocatalytic system. The cooperation of the two sites is essential in the O–O bond formation which occurs at the inter-phase of the Co oxide particle and TiO_2 support.

As featured in:

See Bartłomiej M. Szyja and Rutger A. van Santen, *Phys. Chem. Chem. Phys.*, 2015, **17**, 12486.

ROYAL SOCIETY OF CHEMISTRY

www.rsc.org/pccp

Registered charity number: 207890

PCCP

PAPER

View Article Online
View Journal | View Issue

Cite this: *Phys. Chem. Chem. Phys.*, 2015, **17**, 12486

Received 13th January 2015,
Accepted 24th February 2015

DOI: 10.1039/c5cp00196j

www.rsc.org/pccp

Synergy between TiO_2 and Co_xO_y sites in electrocatalytic water decomposition

Bartłomiej M. Szyja*[a] and Rutger A. van Santen[b]

A computational study of the cooperative effect of a small four-atom Co oxide cluster supported on the TiO_2 anatase (100) surface in the electrochemical water splitting reaction is presented. The results have been obtained including explicit solvent water molecules by means of Car–Parrinello MD simulations. Reaction steps in the catalytic cycle determined involve the formation of TiO_2 surface hydroxyl groups as well as elementary reaction steps on the Co oxide cluster. Essential is the observation of O–O bond formation at the inter-phase of Co oxide particles and the TiO_2 support.

Introduction

The water splitting reaction is an interesting option to store electricity generated by renewable primary energy. It is important from both the economical and environmental points of view. One of the most pursued processes in the case of solar energy conversion there is currently a way to combine electricity generation and hydrolysis in a single system.[1] However, even in the case of separated systems, there is an ongoing effort to improve the characteristics of the catalyst as both electrocatalytic and photochemical processes require the use of appropriate materials in order to provide the satisfactory overall reaction rates. The optimum system for the combined processes has not yet been identified, with the Holy Grail being the catalyst that does not require the over-potential for the reaction to occur, is cheap to obtain and stable under the reaction conditions.

There is a rich experimental[2–6] and computational[7,8] literature on the use of oxidic compounds active as photovoltaic compounds such as TiO_2, Ga_2O_3 or Fe_2O_3. For high activity such systems are usually promoted with metal oxide particles active in oxygen or hydrogen evolution.

A breakthrough in the development of non-noble metal systems for H_2O decomposition was the discovery of the high activity Co phosphate systems by Nocera *et al.*[9] This work has inspired several groups to undertake intensified research in the areas of artificial photosynthesis and solar fuels making use of the abundant species. The activity of different phases of the Co oxide catalysts has been explored computationally by Nørskov *et al.*[10,11] The authors identified the most active phase in the oxygen reduction reaction, that is the β-CoOOH phase, with the value of the over-potential between 0.48 and 0.80 V depending on the surface.

There are many literature reports on the Co_4O_4 cubane unit being active in the water splitting mechanism. The Photosystem II analogue reported by McCool *et al.*[12] is one example of this system coming from the homogeneous catalysis domain. There are also several reports on the cubane unit playing the major role in the water splitting process in heterogeneous catalysis. Du *et al.*[13] elucidated the domain structure of the cobalt oxide water splitting catalyst by means of X-ray pair distribution function analysis. Kanan *et al.*[14] determined the structure and valency of a cobalt-phosphate water oxidation catalyst by means of *in situ* X-ray spectroscopy and demonstrated that cubane structures are likely the active sites in the reaction. This work has been further reviewed by Rosen *et al.*[15] who performed the comparative analysis of the Mg-substituted cubane active sites, and proved that doping of the alkaline metals substantially decreased the activity with respect to oxygen evolution.

Importantly, the group of Nørskov[10,11] indicate that the over-potential in the β-CoOOH system could be reduced by means of doping of single Ni atoms, which is consistent with the experimental work of Trotochaud *et al.*[16] This leads to the question whether there is a synergy between the supporting oxide and the promoting compound. When applied in photo-electrochemical (PEC) systems, the presence of a mixed phase may assist electron–hole separation.[17] A related effect has been suggested for enhanced PEC efficiency of promoted systems that combine photo-excitation with water decomposition.[18]

Anatase TiO_2 is one of the most investigated supports for the metal and metal oxide particles in the field of catalysis, and there are countless examples in both experimental and theoretical

[a] *Institute for Solid State Theory, Univerity of Munster, Wilhelm Klemm Str. 10, 48149 Munster, Germany. E-mail: b.m.szyja@wwu.de*
[b] *Institute for Complex Molecular Systems, Eindhoven University of Technology, Den Dolech 2, 5612AZ Eindhoven, The Netherlands. E-mail: r.a.v.santen@tue.nl*

areas. The original paper of Fujishima and Honda[19] focused on the TiO_2 photocatalyst the one that initiated the research of semiconductor supported particles. The DFT modelling of the small gold nanoparticles on the (101) surface of the anatase has been investigated by the group of Selloni.[20] A similar system containing Pt has been investigated theoretically by Han *et al.*[21] Although these reports cover only the metallic particles, we need to remember that in the OER reaction these small clusters would be present in the oxide form. Other oxides such as the co-catalysts have also been investigated. Kudo *et al.*[22] used NiO_x to improve the catalytic activity. Further details can be found in one of the review papers, for instance, Kudo and Miseki.[23]

The literature on the Co-oxide supported on TiO_2 is limited. The cobalt phosphate "CoPi" oxygen evolution catalyst deposited on titania has been investigated experimentally by Khnayzer *et al.*[24] The cubane structure has been suggested here as well based on XAFS and semiempirical calculations. Interestingly, the overpotential has been determined experimentally to give a value as low as 0.37 V at low pH.

The present study focuses on the electrocatalytic water decomposition on supported active oxide particle system. We will address the question whether synergistic effects may be expected using a computational approach that considers explicitly the role of water.

Model and computational details

For the computational study we have selected a model system consisting of the TiO_2 (100) anatase surface as the support for the Co_4O_4 cluster. The particular TiO_2 surface has been chosen due to its stability[25,26] and its ability to strongly interact with the Co oxide cluster.

We have used 4 atomic layers of anatase TiO_2 that is equivalent to 2 unit cell thickness. The Co_4O_4 cluster was embedded at the valley of the (100) surface with the Co atom connected to the TiO_2 anatase surface *via* oxygen bridges. The lone oxygen atom on Co oxide is pointing upwards. The periodic boundary conditions were imposed in such a way that along the x and y directions the size of the box matched the anatase unit cell size, and the z direction contained a vacuum slab of 13 Å thickness. The water environment has been taken subsequently into account by means of the explicit location of water molecules in the vacuum slab. 64 water molecules have been placed in the system. The geometry has been subsequently equilibrated at 300 K temperature using 1 ps MD run. All calculations have been done using Quantum Espresso ver. 5.0.2. The optimization runs have been carried out using the PWSCF code making use of the PBE functional and 70 Ry cutoff of the plane-wave basis set. For the calculation of the over-potential the Hubbard U parameter was used for Co with a value of 3.3 eV according to the work of Wang *et al.*[27] The Car–Parrinello MD simulations have been carried out using the CPV code with the same functional and cutoff for consistency. The timestep used in simulations was 5 a.u., the electron mass was set to 150 a.u. Each simulation lasted for 80 000 steps that are equivalent to approximately 10 ps. The temperature was kept at 300 K by means of the Nosé–Hoover thermostat.[28,29]

For the needs of the present work it was sufficient to generate one MD trajectory for each electrochemical step. It needs to be pointed out that the factor responsible for the stability of the system is the change in the oxidation state in each particular electrochemical step, which has the reflection in the proton arrangement in the system. The protonation or deprotonation of the particular species occurs *via* the Grotthuss mechanism,[30] and it is fast compared to the simulation time, what has been confirmed by the as-obtained results. In essence, there are only two types of sites that are available for the process – the top Co atom of the cluster and the surface Ti sites, as the Co atoms located at the base of the cluster are fully coordinated and they cannot bind to other species.

There are obviously more surface Ti sites available than the one obtained in the simulation and for which our simulations were carried out. There is a possibility that the change in the oxidation states of each Ti site has a slightly different effect and the location of the hydroxyl species on different Ti sites has a reflection in change in the total energy of the system, but as we stated the proton transfer processes between surface hydroxyls are dynamic and occur during the whole MD run, meaning the energy differences between these different states were below the kT under the assumed simulation conditions. Thus we conclude that differences in stability of the surface Ti–OH species can be neglected.

The procedure used in this work is the same as provided in ref. 34–36 where the reader is referred for details. In general, it is assumed that the reactions occurring at the anode (oxidation) and the cathode (reduction) can be treated as independent processes, and the transfer of the protons and electrons from the anode half-cell to the cathode half-cell is simultaneous. The protons and electrons recombine at the cathode and are in thermodynamic equilibrium with the H_2 molecules formed therein. Thus, the transfer of the proton and the electron can be directly related to the $1/2H_2$ molecule.

The potential of the water splitting reaction is 1.23 V per proton–electron pair transfer. The overall reaction involves 4 such steps, as there are 4 proton–electron pairs needed to form an O_2 molecule. The free energies for each of the reaction steps are calculated using the expression:

$$\Delta G = \Delta G_{\text{product}} - \Delta G_{\text{reactant}} - eU + k_B T \ln a_{H^+}.$$

where ΔG is the free energy of formation of the particular species, U is the potential and a_{H^+} is the activity of the protons. The analogous equations can be formulated for each of the reaction steps. In total the OER requires 4.92 V of the energy input and the over-potential needed to overcome the thermodynamic limitations resulting from the interaction of the intermediate species with the catalyst surface. The theoretical over-potential does not depend on the pH or the potential values, because the free energies obtained by using the above equations vary in the same way as pH and U, thereby the potential determining step remains the same.

Results and discussion

Effect of solvation

Fig. 1 depicts the structure of the Co_4O_4 cluster in the system when the anatase surface is exposed to the vacuum (a) and the water phase (b) respectively. Interestingly, the Co_4O_4 cluster changes its geometry as soon as it comes in contact with water molecules. The water molecule splits into a proton that binds to the lone oxygen atom present at the top of the Co oxide cluster, and a hydroxyl group that binds to the Ti site at the TiO_2 surface. Three other water molecules split in the similar way, the protons coordinate to the oxygen bridges between Co atoms, and the hydroxyl groups bind to the Ti sites at the surface. All these processes take place with water playing a role of the carrier for the OH^- and H^+ species, and so far these were only acid/base reactions, not redox ones.

In addition, two other water molecules coordinate (without splitting) to the top Co atom which changes its coordination number from 4 (tetrahedric) to 6 (octahedric). The remaining Ti sites at the surface coordinate the water molecules as well in a similar fashion. This suggests that there is a slight potential difference on the cluster and on the surface, which might indicate the electron transfer between the two.

This behaviour is different from the one observed previously by Selloni, where only the (001) surface is capable of dissociative water adsorption.[31] In the system investigated in the present work, the dissociation of water is initiated at the cobalt oxide cluster, which – due to the charge imbalance – is able to generate stronger acidic sites, and hydroxyls can bind to the TiO_2 surface.[32]

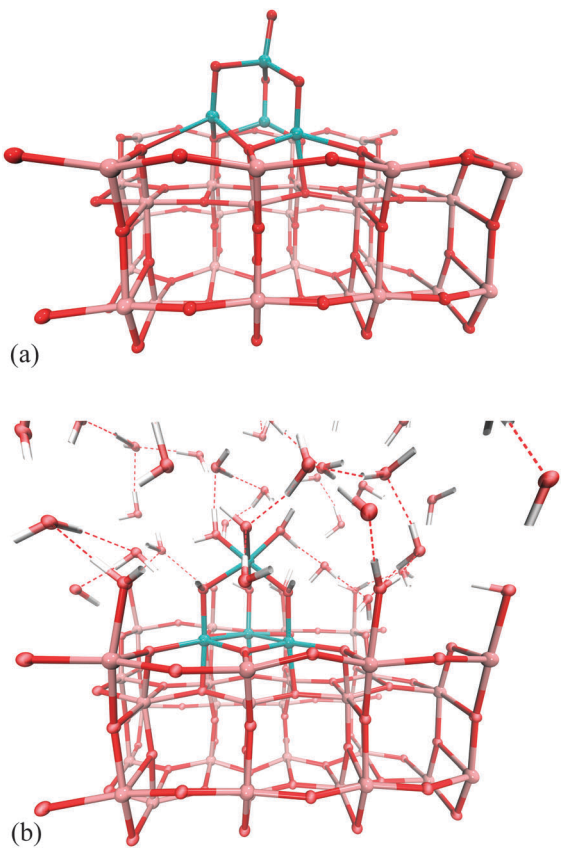

Fig. 1 Geometries of the Co oxide clusters in the gas phase (a) and the water phase (b). Oxygen, titanium, cobalt and hydrogen atoms are shown in red, pink, turquoise and white respectively.

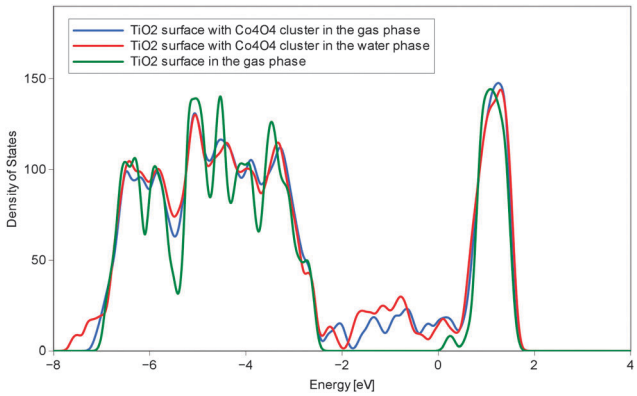

Fig. 2 Gas-phase comparison of valence electron DOS of the pure TiO_2 (100) surface (green) upon the addition of Co_4O_4 (blue). The corresponding structure is shown in Fig. 1a. DOS of the solvated system is shown in red. The corresponding structure is shown in Fig. 1b.

Fig. 2 compares the density of states (DOS) plots of the TiO_2 (100) surface, and the Co_4O_4 cluster on anatase. Consistently with experimental results the pure anatase surface shows the band gap of approximately 3 eV.[33] Upon addition of the Co_4O_4 cluster within the bandgap the additional DOS band of Co_4O_4 appears in the range between −2 and 0 eV. This suggests that when electron holes are generated in the TiO_2 valence band by photon excitation such holes will become stabilized on the Co oxide cluster.

Water dissociation

The simulations of the redox reactions have been done for the anode half reaction of water splitting (the cathode reactions are not covered by this work):

$$2H_2O \rightarrow O_2 + 4H^+ + 4e^- \quad (1)$$

The H_2O decomposition reaction is done according to the procedure presented in ref. 34–36. The overall reaction is split into 4 particular electrochemical steps. The protons and the electrons are carried out of the half-cell to the cathode, where they form the hydrogen molecules. Each of the steps has been simulated by the removal of a hydrogen atom from the system leading to the following partial reactions representing each step of the simulation:

$$H_2O \rightarrow OH^{(Ti)} + H^+ + e^- \quad (2)$$

$$H_2O \rightarrow OH^{(Co)} + H^+ + e^- \quad (3)$$

$$OH^{(Ti)} \rightarrow O^{(Ti)} + H^+ + e^- \quad (4)$$

$$OH^{(Co)} + O^{(Ti)} \rightarrow OOH^{(Ti)} \quad (5)$$

$$OOH^{(Ti)} \rightarrow O_2 + H^+ + e^- \quad (6)$$

The removal of the proton in a particular reaction step has always been done in such a way that no particular surface water

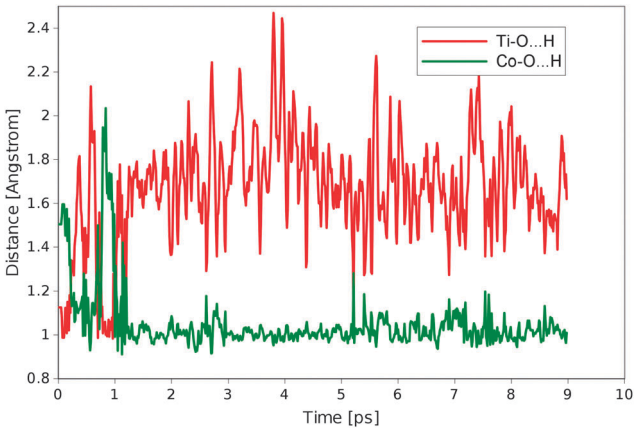

Fig. 3 Distance measured between the O(Co) and the H atom (green line) and O(Ti) and the same H atom (red line) shows the jumping of the H atom between those two sites to finally settle at the O(Co) site at the end of the run.

or hydroxyl species has been affected. The proton was always taken from the bulk water molecule, so another proton from the surface or from the Co oxide cluster could take its place. The system was then allowed to relax to reach the most stable state with respect to the surface hydroxyl configuration. In this way the system always stabilized at the most thermodynamically favoured state and arbitrary selection of the reaction pathway has been avoided.

This approach however raises an issue related to the dynamic nature of the system. The protonation/deprotonation equilibrium between different oxygen sites does not allow the system to settle quickly in one particular state, and during the whole MD run different configurations are observed. The system needs a few picoseconds of time to finally reach the equilibrium with the most stable configuration. This dynamical behaviour is illustrated by Fig. 3.

In reaction (2) the most stable configuration is when the hydroxyl group is formed on the anatase Ti site in addition to the other hydroxyl groups on the surface formed at the solvating stage. The second stage (3) leads to the deprotonation of a water molecule to form the hydroxyl group on the top Co atom. As one hydroxyl group is already bound to this centre, the second hydroxyl group is formed next to it from the coordinated water molecule. This configuration remains relatively stable in the first part of the run, but after approximately 2 ps the water molecule is formed at the Co_4O_4 site as a result of the proton transfer from the surface OH species. This creates a lone oxygen atom at the Ti site of the TiO_2 surface, which is a state resembling the product of reaction (4). This state, however, is only short living because the formal oxidation state of Ti is still unchanged and the electron transfer needed for the electrochemical step has not occurred yet.

Formation of the OOH intermediate (reaction (5)) can occur by the recombination of an OH group with an O atom adsorbed onto the TiO_2 surface. As in the system there are two different OH types of the OH species, the recombination can occur in one of the two ways – either by the transfer of the OH group from the Co_4O_4 cluster, or from the TiO_2 surface, however in both cases the OOH intermediate is adsorbed onto the TiO_2 site. As the implemented protocol involves the removal of the proton and the electron from the system, from the water solvent, the system is allowed to stabilize in the lowest energy configuration. This step, however, cannot be treated with the same approach, because it is not an electrochemical step, and due to the activation barrier it does not occur spontaneously. Thus, the recombination of the OH and O species has been done "manually" – we have constructed the system, where the OH species has been transferred from the Co_4O_4 species. This resulted in the formation of the under-coordinated Co site that during the MD run has been filled with water, and remained in this configuration until the end of the run. If the OH species involved in this recombination was taken from the TiO_2 surface, a similar under-coordinated species would have been formed and filled with water from the solvent phase. The difference between these two options is then the presence of the OH species on the Co or Ti sites. Along with our approach of the assumed rapid equilibration of the location of protons in the system, the most stable configuration should be observed as the result of the proton transfer. We have indeed observed that the water molecule coordinated to the Co_4O_4 site, filling the vacancy after OH species, has been transferred to form the OOH species.

Further evidence to justify this was provided by the NEB transition state search in the isolated system, without the solvent included. The activation barrier calculated for the recombination of the OH species from the Co_4O_4 cluster amounts to 0.87 eV, while for a similar reaction of the TiO_2 surface OH group, the activation energy is higher and amounts to 1.05 eV.

This implies that there is a difference in the relationship between the OH and OOH chemical bonding strength in a mono-functional and the system investigated in this work. This effect is responsible for the relatively low over-potential value obtained, and fully consistent with the doping effect described theoretically and experimentally.[10,11,16]

The final step is the formation of the oxygen molecule by the removal of the hydrogen atom from the peroxide species – reaction (6). This is again the electrochemical step and involves the removal of H^+ and e^-.

The complete set of reaction intermediates, including all steps, is shown in Fig. 4.

Over-potential

The energetics of this reaction is really challenging to calculate in the explicit solvent approach. Due to the many hydrogen bonds present in the system and dynamic equilibrium of the surface hydroxyl species, the potential energy fluctuates significantly along the run. The energy values of relevance are of the order of tenths of eV or even less and the accuracy of the CPMD simulations is not able to calculate the energy with this accuracy. Instead we have decided to follow the gas phase approach for the calculation of the over-potential, which is similar to that described in ref. 10. At the end of each MD

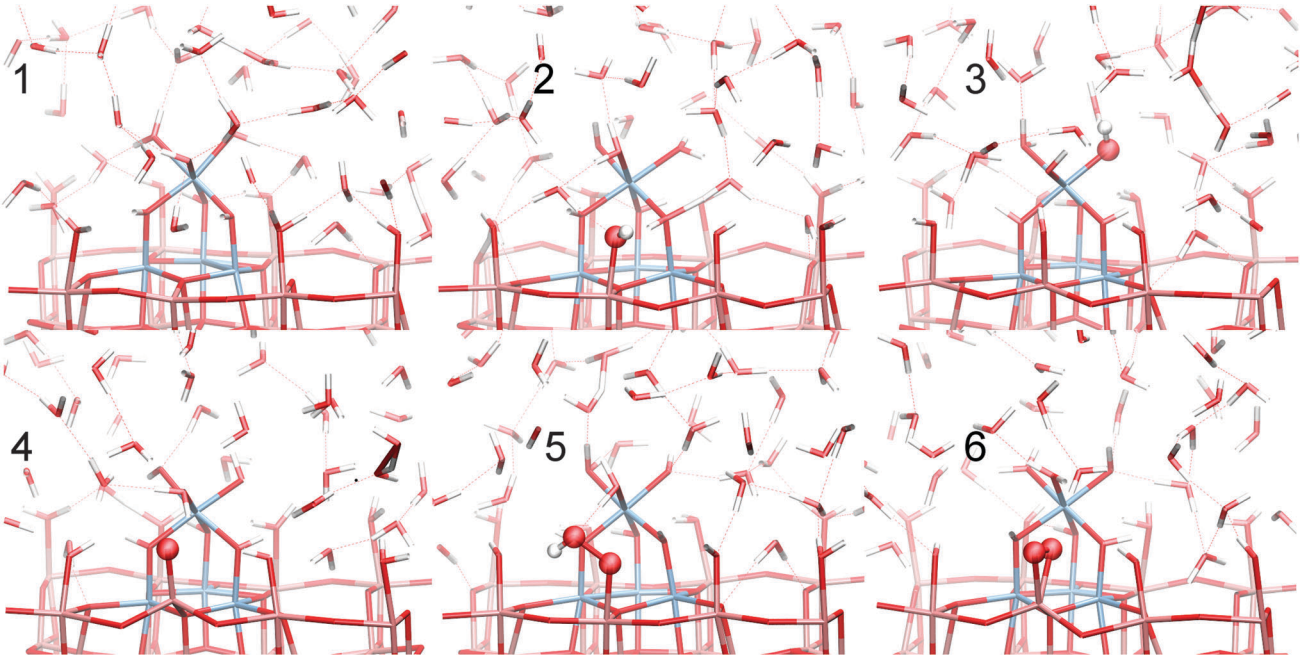

Fig. 4 Intermediate stages of water electroreduction. The titanium, cobalt, oxygen and hydrogen atoms are marked in pink, blue, red and white respectively. The states involved in the particular reaction step are shown in ball-and-stick representation. Hydrogen bonds are marked with thin dashed lines.

simulation we have determined the most stable configuration of the system and from this system we have removed all water molecules. This in essence gives us back the systems prior to the introduction of water molecules, but with the surface of the anatase that is appropriately hydroxylated and the Co_4O_4 cluster protonated. For these geometries we have calculated the electronic energy and performed the vibrational analysis to calculate the ZPE of all surface hydroxyl species and top layer anatase atoms. Prior to that, the systems representing each step of the electrochemical half reactions have been relaxed to reach the forces smaller than 0.001 eV $Å^{-1}$. The energetic diagram of the whole process is shown in Fig. 5.

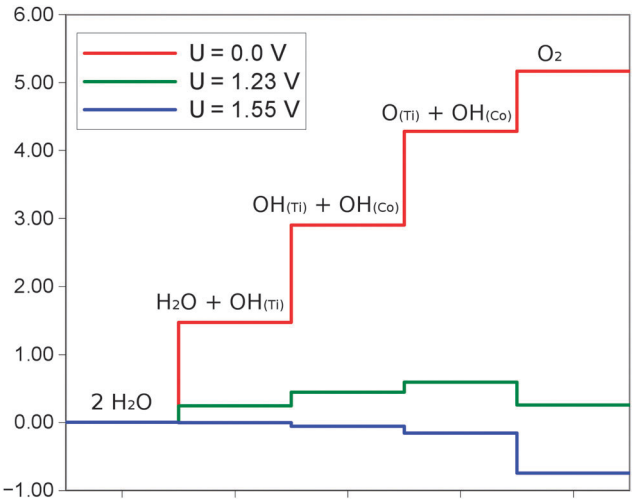

Fig. 5 Overpotential for the calculated reaction steps.

The rate limiting step is the first electrochemical step of the process – reaction (3) – where the first hydroxyl is formed out of the water molecule at the surface Ti site. The estimated over-potential amounts to 0.32 eV. This value is lower than the one obtained by the group of Nørskov (0.48 V) for the β-CoOOH phase,[10,11] and is another indication of the cooperative effect between the sites. It is also consistent with the finding of Trotochaud *et al.*[16] on the effect of doping of pure surfaces.

Interestingly, this value is very close to experimental observations of Khnayzer *et al.*[24] for the cobalt phosphate cluster supported on titania, where at low pH the over-potential has been determined to be 0.37 V.

Conclusions

The main density of states of the hydroxylated Co_4O_4 cluster is located within the energy gap between the valence and conduction bands of the anatase surface (100) studied. This allows it to be a catalytically active component of the water decomposition reaction of the photocatalytic system. The unoccupied d-atomic orbital LDOS of Co states can accept an electron from the TiO_2 conduction band. Alternatively, a hole in the TiO_2 valence band will recombine with the electron from the occupied Co d-valence band.

The sites on the Co cluster and the TiO_2 surface have a cooperative interaction in the electrocatalytic H_2O decomposition reaction, the Co_4O_4 cluster initially becomes protonated and the hydroxyl groups will bind to the TiO_2 surface. To explicitly include the solvent molecules is essential for this step – water molecules assist in the redistribution of the protons and hydroxyls between the TiO_2 support and the Co_4O_4 cluster.

In the peroxide formation step, O adsorbed onto the TiO_2 surface recombines with the OH species from the Co_4O_4 cluster.

The over-potential calculated for this system amounts to 0.32 V and represents the potential needed to form the hydroxyl species on the surface Ti site.

Acknowledgements

The calculations have been carried out using the *Cartesius* supercomputer at SURFsara. The computational grant from NCF number SH-203-11 is gratefully acknowledged. The VMD program[37] has been used to perform the MD analyses and prepare the images of structures.

Notes and references

1 N. L. Panwar, S. C. Kaushik and S. Kothari, *Renewable Sustainable Energy Rev.*, 2011, **15**, 1513.
2 L. Meng, C. Li and M. P. dos Santos, *J. Inorg. Organomet. Polym. Mater.*, 2013, **23**, 787.
3 C. Yang, M. Li, W.-H. Zhang and C. Li, *Sol. Energy Mater. Sol. Cells*, 2013, **115**, 100.
4 X. Zheng, D. Yu, F.-Q. Xiong, M. Li, Z. Yang, J. Zhu, W.-H. Zhang and C. Li, *Chem. Commun.*, 2014, **50**, 4364.
5 K. Maeda, M. Higashi, B. Siritanaratkul, R. Abe and K. Domen, *J. Am. Chem. Soc.*, 2011, **133**, 12334.
6 J. Kubota and K. Domen, *Electrochem. Soc. Interface*, 2013, 57.
7 Á. Valdés, J. Brillet, M. Grätzel, H. Gudmundsdóttir, H. A. Hansen, H. Jónsson, P. Klüpfel, G.-J. Kroes, F. Le Formal, I. C. Man, R. S. Martins, J. K. Nørskov, J. Rossmeisl, K. Sivula, A. Vojvodic and M. Zäch, *Phys. Chem. Chem. Phys.*, 2012, **14**, 49.
8 Á. Valdés and G.-J. Kroes, *J. Phys. Chem. C*, 2010, **114**, 1701.
9 A. J. Esswein, Y. Surendranath, S. Y. Reece and D. G. Nocera, *Energy Environ. Sci.*, 2011, **4**, 499.
10 M. Bajdich, M. García-Mota, A. Vojvodic, J. K. Nørskov and A. T. Bell, *J. Am. Chem. Soc.*, 2013, **135**, 13521.
11 M. García-Mota, M. Bajdich, V. Viswanathan, A. Vojvodic, A. T. Bell and J. K. Nørskov, *J. Phys. Chem. C*, 2012, **116**, 21077.
12 N. S. McCool, D. M. Robinson, J. E. Sheats and G. C. Dismukes, *J. Am. Chem. Soc.*, 2011, **133**, 11446.
13 P. Du, O. Kokhan, K. W. Chapman, P. J. Chupas and D. M. Tiede, *J. Am. Chem. Soc.*, 2012, **134**, 11096.
14 M. W. Kanan, J. Yano, Y. Surendranath, M. Dincă, V. K. Yachandra and D. G. Nocera, *J. Am. Chem. Soc.*, 2010, **132**, 13692.
15 J. Rosen, G. S. Hutchings and F. Jiao, *J. Am. Chem. Soc.*, 2013, **135**, 4516.
16 L. Trotochaud, J. K. Ranney, K. N. Williams and S. W. Boettcher, *J. Am. Chem. Soc.*, 2012, **134**, 17253.
17 R. Li, F. Zhang, D. Wang, J. Yang, M. Li, J. Zhu, X. Zhou, H. Han and C. Li, *Nat. Commun.*, 2013, **4**, 1432.
18 X. Wang, Q. Xu, M. Li, S. Shen, X. Wang, Y. Wang, Z. Feng, J. Shi, H. Han and C. Li, *Angew. Chem., Int. Ed.*, 2012, **51**, 13089.
19 A. Fujishima and K. Honda, *Nature*, 1972, **238**, 37.
20 A. Vittadini and A. Selloni, *J. Chem. Phys.*, 2002, **117**, 353.
21 Y. Han, C.-J. Liu and Q. Ge, *J. Phys. Chem. B*, 2006, **110**, 7463.
22 A. Kudo, K. Domen, K. Maruya and T. Onishi, *Chem. Phys. Lett.*, 1987, **133**, 517.
23 A. Kudo and Y. Miseki, *Chem. Soc. Rev.*, 2009, **38**, 253.
24 R. S. Khnayzer, M. W. Mara, J. Huang, M. L. Shelby, L. X. Chen and F. N. Castellano, *ACS Catal.*, 2012, **2**, 2150.
25 M. Lazzeri, A. Vittadini and A. Selloni, *Phys. Rev. B: Condens. Matter Mater. Phys.*, 2001, **63**, 155409.
26 M. Lazzeri, A. Vittadini and A. Selloni, *Phys. Rev. B: Condens. Matter Mater. Phys.*, 2003, **65**, 119901.
27 L. Wang, Th. Maxisch and G. Ceder, *Phys. Rev. B: Condens. Matter Mater. Phys.*, 2006, **73**, 195107.
28 S. Nosé, *J. Chem. Phys.*, 1984, **81**, 511.
29 W. G. Hoover, *Phys. Rev. A: At., Mol., Opt. Phys.*, 1985, **31**, 1695.
30 C. J. T. de Grotthuss, *Ann. Chim.*, 1806, **58**, 54.
31 A. Selloni, *Nat. Mater.*, 2008, **7**, 613.
32 A. Vittadini, A. Selloni, F. P. Rotzinger and M. Grätzel, *Phys. Rev. Lett.*, 1998, **81**, 2954.
33 K. M. Reddy, S. V. Manorama and A. R. Reddy, *Mater. Chem. Phys.*, 2002, **78**, 239.
34 J. Rossmeisl, A. Logadottir and J. K. Norskov, *Chem. Phys.*, 2005, **319**, 178.
35 J. Rossmeisl, Z. W. Qu, H. Zhu, G. J. Kroes and J. K. Norskov, *J. Electroanal. Chem.*, 2007, **607**, 83.
36 H. A. Hansen, I. C. Man, F. Studt, F. Abild-Pedersen, T. Bligaard and J. Rossmeisl, *Phys. Chem. Chem. Phys.*, 2010, **12**, 283.
37 W. Humphrey, A. Dalke and K. Schulten, *J. Mol. Graphics*, 1996, **14**, 33.